FERMILAB-PUB-06-089-E

Search for R-parity violating supersymmetry via the $LL\bar{E}$ couplings λ_{121}, λ_{122} or λ_{133} in $p\bar{p}$ collisions at $\sqrt{s} = 1.96$ TeV

V.M. Abazov,[36] B. Abbott,[76] M. Abolins,[66] B.S. Acharya,[29] M. Adams,[52] T. Adams,[50] M. Agelou,[18] J.-L. Agram,[19] S.H. Ahn,[31] M. Ahsan,[60] G.D. Alexeev,[36] G. Alkhazov,[40] A. Alton,[65] G. Alverson,[64] G.A. Alves,[2] M. Anastasoaie,[35] T. Andeen,[54] S. Anderson,[46] B. Andrieu,[17] M.S. Anzelc,[54] Y. Arnoud,[14] M. Arov,[53] A. Askew,[50] B. Åsman,[41] A.C.S. Assis Jesus,[3] O. Atramentov,[58] C. Autermann,[21] C. Avila,[8] C. Ay,[24] F. Badaud,[13] A. Baden,[62] L. Bagby,[53] B. Baldin,[51] D.V. Bandurin,[59] P. Banerjee,[29] S. Banerjee,[29] E. Barberis,[64] P. Bargassa,[81] P. Baringer,[59] C. Barnes,[44] J. Barreto,[2] J.F. Bartlett,[51] U. Bassler,[17] D. Bauer,[44] A. Bean,[59] M. Begalli,[3] M. Begel,[72] C. Belanger-Champagne,[5] L. Bellantoni,[51] A. Bellavance,[68] J.A. Benitez,[66] S.B. Beri,[27] G. Bernardi,[17] R. Bernhard,[42] L. Berntzon,[15] I. Bertram,[43] M. Besançon,[18] R. Beuselinck,[44] V.A. Bezzubov,[39] P.C. Bhat,[51] V. Bhatnagar,[27] M. Binder,[25] C. Biscarat,[43] K.M. Black,[63] I. Blackler,[44] G. Blazey,[53] F. Blekman,[44] S. Blessing,[50] D. Bloch,[19] K. Bloom,[68] U. Blumenschein,[23] A. Boehnlein,[51] O. Boeriu,[56] T.A. Bolton,[60] F. Borcherding,[51] G. Borissov,[43] K. Bos,[34] T. Bose,[78] A. Brandt,[79] R. Brock,[66] G. Brooijmans,[71] A. Bross,[51] D. Brown,[79] N.J. Buchanan,[50] D. Buchholz,[54] M. Buehler,[82] V. Buescher,[23] S. Burdin,[51] S. Burke,[46] T.H. Burnett,[83] E. Busato,[17] C.P. Buszello,[44] J.M. Butler,[63] P. Calfayan,[25] S. Calvet,[15] J. Cammin,[72] S. Caron,[34] W. Carvalho,[3] B.C.K. Casey,[78] N.M. Cason,[56] H. Castilla-Valdez,[33] S. Chakrabarti,[29] D. Chakraborty,[53] K.M. Chan,[72] A. Chandra,[49] D. Chapin,[78] F. Charles,[19] E. Cheu,[46] F. Chevallier,[14] D.K. Cho,[63] S. Choi,[32] B. Choudhary,[28] L. Christofek,[59] D. Claes,[68] B. Clément,[19] C. Clément,[41] Y. Coadou,[5] M. Cooke,[81] W.E. Cooper,[51] D. Coppage,[59] M. Corcoran,[81] M.-C. Cousinou,[15] B. Cox,[45] S. Crépé-Renaudin,[14] D. Cutts,[78] M. Ćwiok,[30] H. da Motta,[2] A. Das,[63] M. Das,[61] B. Davies,[43] G. Davies,[44] G.A. Davis,[54] K. De,[79] P. de Jong,[34] S.J. de Jong,[35] E. De La Cruz-Burelo,[65] C. De Oliveira Martins,[3] J.D. Degenhardt,[65] F. Déliot,[18] M. Demarteau,[51] R. Demina,[72] P. Demine,[18] D. Denisov,[51] S.P. Denisov,[39] S. Desai,[73] H.T. Diehl,[51] M. Diesburg,[51] M. Doidge,[43] A. Dominguez,[68] H. Dong,[73] L.V. Dudko,[38] L. Duflot,[16] S.R. Dugad,[29] A. Duperrin,[15] J. Dyer,[66] A. Dyshkant,[53] M. Eads,[68] D. Edmunds,[66] T. Edwards,[45] J. Ellison,[49] J. Elmsheuser,[25] V.D. Elvira,[51] S. Eno,[62] P. Ermolov,[38] J. Estrada,[51] H. Evans,[55] A. Evdokimov,[37] V.N. Evdokimov,[39] S.N. Fatakia,[63] L. Feligioni,[63] A.V. Ferapontov,[60] T. Ferbel,[72] F. Fiedler,[25] F. Filthaut,[35] W. Fisher,[51] H.E. Fisk,[51] I. Fleck,[23] M. Ford,[45] M. Fortner,[53] H. Fox,[23] S. Fu,[51] S. Fuess,[51] T. Gadfort,[83] C.F. Galea,[35] E. Gallas,[51] E. Galyaev,[56] C. Garcia,[72] A. Garcia-Bellido,[83] J. Gardner,[59] V. Gavrilov,[37] A. Gay,[19] P. Gay,[13] D. Gelé,[19] R. Gelhaus,[49] C.E. Gerber,[52] Y. Gershtein,[50] D. Gillberg,[5] G. Ginther,[72] N. Gollub,[41] B. Gómez,[8] K. Gounder,[51] A. Goussiou,[56] P.D. Grannis,[73] H. Greenlee,[51] Z.D. Greenwood,[61] E.M. Gregores,[4] G. Grenier,[20] Ph. Gris,[13] J.-F. Grivaz,[16] S. Grünendahl,[51] M.W. Grünewald,[30] F. Guo,[73] J. Guo,[73] G. Gutierrez,[51] P. Gutierrez,[76] A. Haas,[71] N.J. Hadley,[62] P. Haefner,[25] S. Hagopian,[50] J. Haley,[69] I. Hall,[76] R.E. Hall,[48] L. Han,[7] K. Hanagaki,[51] K. Harder,[60] A. Harel,[72] R. Harrington,[64] J.M. Hauptman,[58] R. Hauser,[66] J. Hays,[54] T. Hebbeker,[21] D. Hedin,[53] J.G. Hegeman,[34] J.M. Heinmiller,[52] A.P. Heinson,[49] U. Heintz,[63] C. Hensel,[59] G. Hesketh,[64] M.D. Hildreth,[56] R. Hirosky,[82] J.D. Hobbs,[73] B. Hoeneisen,[12] H. Hoeth,[26] M. Hohlfeld,[16] S.J. Hong,[31] R. Hooper,[78] P. Houben,[34] Y. Hu,[73] Z. Hubacek,[10] V. Hynek,[9] I. Iashvili,[70] R. Illingworth,[51] A.S. Ito,[51] S. Jabeen,[63] M. Jaffré,[16] S. Jain,[76] K. Jakobs,[23] C. Jarvis,[62] A. Jenkins,[44] R. Jesik,[44] K. Johns,[46] C. Johnson,[71] M. Johnson,[51] A. Jonckheere,[51] P. Jonsson,[44] A. Juste,[51] D. Käfer,[21] S. Kahn,[74] E. Kajfasz,[15] A.M. Kalinin,[36] J.M. Kalk,[61] J.R. Kalk,[66] S. Kappler,[21] D. Karmanov,[38] J. Kasper,[63] P. Kasper,[51] I. Katsanos,[71] D. Kau,[50] R. Kaur,[27] R. Kehoe,[80] S. Kermiche,[15] S. Kesisoglou,[78] N. Khalatyan,[63] A. Khanov,[77] A. Kharchilava,[70] Y.M. Kharzheev,[36] D. Khatidze,[71] H. Kim,[79] T.J. Kim,[31] M.H. Kirby,[35] B. Klima,[51] J.M. Kohli,[27] J.-P. Konrath,[23] M. Kopal,[76] V.M. Korablev,[39] J. Kotcher,[74] B. Kothari,[71] A. Koubarovsky,[38] A.V. Kozelov,[39] J. Kozminski,[66] A. Kryemadhi,[82] S. Krzywdzinski,[51] T. Kuhl,[24] A. Kumar,[70] S. Kunori,[62] A. Kupco,[11] T. Kurča,[20,*] J. Kvita,[9] S. Lager,[41] S. Lammers,[71] G. Landsberg,[78] J. Lazoflores,[50] A.-C. Le Bihan,[19] P. Lebrun,[20] W.M. Lee,[53] A. Leflat,[38] F. Lehner,[42] V. Lesne,[13] J. Leveque,[46] P. Lewis,[44] J. Li,[79] Q.Z. Li,[51] J.G.R. Lima,[53] D. Lincoln,[51] J. Linnemann,[66] V.V. Lipaev,[39] R. Lipton,[51] Z. Liu,[5] L. Lobo,[44] A. Lobodenko,[40] M. Lokajicek,[11] A. Lounis,[19] P. Love,[43] H.J. Lubatti,[83] M. Lynker,[56] A.L. Lyon,[51] A.K.A. Maciel,[2] R.J. Madaras,[47] P. Mättig,[26] C. Magass,[21] A. Magerkurth,[65] A.-M. Magnan,[14] N. Makovec,[16] P.K. Mal,[56] H.B. Malbouisson,[3] S. Malik,[68] V.L. Malyshev,[36] H.S. Mao,[6] Y. Maravin,[60] M. Martens,[51] S.E.K. Mattingly,[78] R. McCarthy,[73] R. McCroskey,[46] D. Meder,[24] A. Melnitchouk,[67] A. Mendes,[15] L. Mendoza,[8] M. Merkin,[38] K.W. Merritt,[51] A. Meyer,[21] J. Meyer,[22] M. Michaut,[18] H. Miettinen,[81] T. Millet,[20] J. Mitrevski,[71] J. Molina,[3] N.K. Mondal,[29] J. Monk,[45] R.W. Moore,[5] T. Moulik,[59] G.S. Muanza,[16] M. Mulders,[51] M. Mulhearn,[71] L. Mundim,[3] Y.D. Mutaf,[73] E. Nagy,[15]

M. Naimuddin,[28] M. Narain,[63] N.A. Naumann,[35] H.A. Neal,[65] J.P. Negret,[8] S. Nelson,[50] P. Neustroev,[40] C. Noeding,[23] A. Nomerotski,[51] S.F. Novaes,[4] T. Nunnemann,[25] V. O'Dell,[51] D.C. O'Neil,[5] G. Obrant,[40] V. Oguri,[3] N. Oliveira,[3] N. Oshima,[51] R. Otec,[10] G.J. Otero y Garzón,[52] M. Owen,[45] P. Padley,[81] N. Parashar,[57] S.-J. Park,[72] S.K. Park,[31] J. Parsons,[71] R. Partridge,[78] N. Parua,[73] A. Patwa,[74] G. Pawloski,[81] P.M. Perea,[49] E. Perez,[18] K. Peters,[45] P. Pétroff,[16] M. Petteni,[44] R. Piegaia,[1] M.-A. Pleier,[22] P.L.M. Podesta-Lerma,[33] V.M. Podstavkov,[51] Y. Pogorelov,[56] M.-E. Pol,[2] A. Pompoš,[76] B.G. Pope,[66] A.V. Popov,[39] W.L. Prado da Silva,[3] H.B. Prosper,[50] S. Protopopescu,[74] J. Qian,[65] A. Quadt,[22] B. Quinn,[67] K.J. Rani,[29] K. Ranjan,[28] P.A. Rapidis,[51] P.N. Ratoff,[43] P. Renkel,[80] S. Reucroft,[64] M. Rijssenbeek,[73] I. Ripp-Baudot,[19] F. Rizatdinova,[77] S. Robinson,[44] R.F. Rodrigues,[3] C. Royon,[18] P. Rubinov,[51] R. Ruchti,[56] V.I. Rud,[38] G. Sajot,[14] A. Sánchez-Hernández,[33] M.P. Sanders,[62] A. Santoro,[3] G. Savage,[51] L. Sawyer,[61] T. Scanlon,[44] D. Schaile,[25] R.D. Schamberger,[73] Y. Scheglov,[40] H. Schellman,[54] P. Schieferdecker,[25] C. Schmitt,[26] C. Schwanenberger,[45] A. Schwartzman,[69] R. Schwienhorst,[66] S. Sengupta,[50] H. Severini,[76] E. Shabalina,[52] M. Shamim,[60] V. Shary,[18] A.A. Shchukin,[39] W.D. Shephard,[56] R.K. Shivpuri,[28] D. Shpakov,[64] V. Siccardi,[19] R.A. Sidwell,[60] V. Simak,[10] V. Sirotenko,[51] P. Skubic,[76] P. Slattery,[72] R.P. Smith,[51] G.R. Snow,[68] J. Snow,[75] S. Snyder,[74] S. Söldner-Rembold,[45] X. Song,[53] L. Sonnenschein,[17] A. Sopczak,[43] M. Sosebee,[79] K. Soustruznik,[9] M. Souza,[2] B. Spurlock,[79] J. Stark,[14] J. Steele,[61] K. Stevenson,[55] V. Stolin,[37] A. Stone,[52] D.A. Stoyanova,[39] J. Strandberg,[41] M.A. Strang,[70] M. Strauss,[76] R. Ströhmer,[25] D. Strom,[54] M. Strovink,[47] L. Stutte,[51] S. Sumowidagdo,[50] A. Sznajder,[3] M. Talby,[15] P. Tamburello,[46] W. Taylor,[5] P. Telford,[45] J. Temple,[46] B. Tiller,[25] M. Titov,[23] V.V. Tokmenin,[36] M. Tomoto,[51] T. Toole,[62] I. Torchiani,[23] S. Towers,[43] T. Trefzger,[24] S. Trincaz-Duvoid,[17] D. Tsybychev,[73] B. Tuchming,[18] C. Tully,[69] A.S. Turcot,[45] P.M. Tuts,[71] R. Unalan,[66] L. Uvarov,[40] S. Uvarov,[40] S. Uzunyan,[53] B. Vachon,[5] P.J. van den Berg,[34] R. Van Kooten,[55] W.M. van Leeuwen,[34] N. Varelas,[52] E.W. Varnes,[46] A. Vartapetian,[79] I.A. Vasilyev,[39] M. Vaupel,[26] P. Verdier,[20] L.S. Vertogradov,[36] M. Verzocchi,[51] F. Villeneuve-Seguier,[44] P. Vint,[44] J.-R. Vlimant,[17] E. Von Toerne,[60] M. Voutilainen,[68,†] M. Vreeswijk,[34] H.D. Wahl,[50] L. Wang,[62] J. Warchol,[56] G. Watts,[83] M. Wayne,[56] M. Weber,[51] H. Weerts,[66] N. Wermes,[22] M. Wetstein,[62] A. White,[79] D. Wicke,[26] G.W. Wilson,[59] S.J. Wimpenny,[49] M. Wobisch,[51] J. Womersley,[51] D.R. Wood,[64] T.R. Wyatt,[45] Y. Xie,[78] N. Xuan,[56] S. Yacoob,[54] R. Yamada,[51] M. Yan,[62] T. Yasuda,[51] Y.A. Yatsunenko,[36] K. Yip,[74] H.D. Yoo,[78] S.W. Youn,[54] C. Yu,[14] J. Yu,[79] A. Yurkewicz,[73] A. Zatserklyaniy,[53] C. Zeitnitz,[26] D. Zhang,[51] T. Zhao,[83] Z. Zhao,[65] B. Zhou,[65] J. Zhu,[73] M. Zielinski,[72] D. Zieminska,[55] A. Zieminski,[55] V. Zutshi,[53] and E.G. Zverev[38]

(DØ Collaboration)

[1] *Universidad de Buenos Aires, Buenos Aires, Argentina*
[2] *LAFEX, Centro Brasileiro de Pesquisas Físicas, Rio de Janeiro, Brazil*
[3] *Universidade do Estado do Rio de Janeiro, Rio de Janeiro, Brazil*
[4] *Instituto de Física Teórica, Universidade Estadual Paulista, São Paulo, Brazil*
[5] *University of Alberta, Edmonton, Alberta, Canada, Simon Fraser University, Burnaby, British Columbia, Canada, York University, Toronto, Ontario, Canada, and McGill University, Montreal, Quebec, Canada*
[6] *Institute of High Energy Physics, Beijing, People's Republic of China*
[7] *University of Science and Technology of China, Hefei, People's Republic of China*
[8] *Universidad de los Andes, Bogotá, Colombia*
[9] *Center for Particle Physics, Charles University, Prague, Czech Republic*
[10] *Czech Technical University, Prague, Czech Republic*
[11] *Center for Particle Physics, Institute of Physics, Academy of Sciences of the Czech Republic, Prague, Czech Republic*
[12] *Universidad San Francisco de Quito, Quito, Ecuador*
[13] *Laboratoire de Physique Corpusculaire, IN2P3-CNRS, Université Blaise Pascal, Clermont-Ferrand, France*
[14] *Laboratoire de Physique Subatomique et de Cosmologie, IN2P3-CNRS, Universite de Grenoble 1, Grenoble, France*
[15] *CPPM, IN2P3-CNRS, Université de la Méditerranée, Marseille, France*
[16] *IN2P3-CNRS, Laboratoire de l'Accélérateur Linéaire, Orsay, France*
[17] *LPNHE, IN2P3-CNRS, Universités Paris VI and VII, Paris, France*
[18] *DAPNIA/Service de Physique des Particules, CEA, Saclay, France*
[19] *IReS, IN2P3-CNRS, Université Louis Pasteur, Strasbourg, France, and Université de Haute Alsace, Mulhouse, France*
[20] *Institut de Physique Nucléaire de Lyon, IN2P3-CNRS, Université Claude Bernard, Villeurbanne, France*
[21] *III. Physikalisches Institut A, RWTH Aachen, Aachen, Germany*
[22] *Physikalisches Institut, Universität Bonn, Bonn, Germany*
[23] *Physikalisches Institut, Universität Freiburg, Freiburg, Germany*
[24] *Institut für Physik, Universität Mainz, Mainz, Germany*
[25] *Ludwig-Maximilians-Universität München, München, Germany*
[26] *Fachbereich Physik, University of Wuppertal, Wuppertal, Germany*
[27] *Panjab University, Chandigarh, India*
[28] *Delhi University, Delhi, India*

[29] *Tata Institute of Fundamental Research, Mumbai, India*
[30] *University College Dublin, Dublin, Ireland*
[31] *Korea Detector Laboratory, Korea University, Seoul, Korea*
[32] *SungKyunKwan University, Suwon, Korea*
[33] *CINVESTAV, Mexico City, Mexico*
[34] *FOM-Institute NIKHEF and University of Amsterdam/NIKHEF, Amsterdam, The Netherlands*
[35] *Radboud University Nijmegen/NIKHEF, Nijmegen, The Netherlands*
[36] *Joint Institute for Nuclear Research, Dubna, Russia*
[37] *Institute for Theoretical and Experimental Physics, Moscow, Russia*
[38] *Moscow State University, Moscow, Russia*
[39] *Institute for High Energy Physics, Protvino, Russia*
[40] *Petersburg Nuclear Physics Institute, St. Petersburg, Russia*
[41] *Lund University, Lund, Sweden, Royal Institute of Technology and Stockholm University, Stockholm, Sweden, and Uppsala University, Uppsala, Sweden*
[42] *Physik Institut der Universität Zürich, Zürich, Switzerland*
[43] *Lancaster University, Lancaster, United Kingdom*
[44] *Imperial College, London, United Kingdom*
[45] *University of Manchester, Manchester, United Kingdom*
[46] *University of Arizona, Tucson, Arizona 85721, USA*
[47] *Lawrence Berkeley National Laboratory and University of California, Berkeley, California 94720, USA*
[48] *California State University, Fresno, California 93740, USA*
[49] *University of California, Riverside, California 92521, USA*
[50] *Florida State University, Tallahassee, Florida 32306, USA*
[51] *Fermi National Accelerator Laboratory, Batavia, Illinois 60510, USA*
[52] *University of Illinois at Chicago, Chicago, Illinois 60607, USA*
[53] *Northern Illinois University, DeKalb, Illinois 60115, USA*
[54] *Northwestern University, Evanston, Illinois 60208, USA*
[55] *Indiana University, Bloomington, Indiana 47405, USA*
[56] *University of Notre Dame, Notre Dame, Indiana 46556, USA*
[57] *Purdue University Calumet, Hammond, Indiana 46323, USA*
[58] *Iowa State University, Ames, Iowa 50011, USA*
[59] *University of Kansas, Lawrence, Kansas 66045, USA*
[60] *Kansas State University, Manhattan, Kansas 66506, USA*
[61] *Louisiana Tech University, Ruston, Louisiana 71272, USA*
[62] *University of Maryland, College Park, Maryland 20742, USA*
[63] *Boston University, Boston, Massachusetts 02215, USA*
[64] *Northeastern University, Boston, Massachusetts 02115, USA*
[65] *University of Michigan, Ann Arbor, Michigan 48109, USA*
[66] *Michigan State University, East Lansing, Michigan 48824, USA*
[67] *University of Mississippi, University, Mississippi 38677, USA*
[68] *University of Nebraska, Lincoln, Nebraska 68588, USA*
[69] *Princeton University, Princeton, New Jersey 08544, USA*
[70] *State University of New York, Buffalo, New York 14260, USA*
[71] *Columbia University, New York, New York 10027, USA*
[72] *University of Rochester, Rochester, New York 14627, USA*
[73] *State University of New York, Stony Brook, New York 11794, USA*
[74] *Brookhaven National Laboratory, Upton, New York 11973, USA*
[75] *Langston University, Langston, Oklahoma 73050, USA*
[76] *University of Oklahoma, Norman, Oklahoma 73019, USA*
[77] *Oklahoma State University, Stillwater, Oklahoma 74078, USA*
[78] *Brown University, Providence, Rhode Island 02912, USA*
[79] *University of Texas, Arlington, Texas 76019, USA*
[80] *Southern Methodist University, Dallas, Texas 75275, USA*
[81] *Rice University, Houston, Texas 77005, USA*
[82] *University of Virginia, Charlottesville, Virginia 22901, USA*
[83] *University of Washington, Seattle, Washington 98195, USA*

(Dated: April 30, 2006)

A search for gaugino pair production with a trilepton signature in the framework of R-parity violating supersymmetry via the couplings λ_{121}, λ_{122}, or λ_{133} is presented. The data, corresponding to an integrated luminosity of $\mathcal{L} \approx 360$ pb^{-1}, were collected from April 2002 to August 2004 with the DØ detector at the Fermilab Tevatron Collider, at a center-of-mass energy of $\sqrt{s} = 1.96$ TeV. This analysis considers final states with three charged leptons with the flavor combinations $ee\ell$, $\mu\mu\ell$,

and $ee\tau$ ($\ell = e$ or μ). No evidence for supersymmetry is found and limits at the 95% confidence level are set on the gaugino pair production cross section and lower bounds on the masses of the lightest neutralino and chargino are derived in two supersymmetric models.

PACS numbers: 11.30.Pb Supersymmetry, 04.65.+e Supergravity, 12.60.Jv Supersymmetric models

Supersymmetry (SUSY) [1] predicts the existence of a new particle for each standard model (SM) particle, differing by half a unit in spin but otherwise sharing the same quantum numbers. The new scalar particles, known as squarks and sleptons, carry baryon (B) or lepton (L) quantum numbers, potentially leading to interactions violating B or L conservation. In the supersymmetric Lagrangian, there is a continuous R-invariance, which prevents lepton and baryon number violation, but also prevents gluinos and gravitinos from being massive.

In a supergravity scenario, the gravitino will acquire mass through the spontaneous breaking of local SUSY. The SUSY-breaking is then communicated to the so-called observable sector so that, in particular, the gluino acquires its mass [2]. This breaks the continuous R-invariance, leaving only a discrete version, which is called R-parity [3]. Each particle is characterized by an R-parity quantum number defined as $R_p = (-1)^{3B+L+2S}$ (S being the spin), such that SM particles have $R_p = 1$ and SUSY particles $R_p = -1$. The gauge symmetry allows R-parity violating ($\not{R}_p$) terms to be included in the superpotential [4]. These terms are:

$$W_{\not{R}_p} = +\frac{1}{2}\lambda_{ijk}\, L_i L_j \bar{E}_k + \lambda'_{ijk}\, L_i Q_j \bar{D}_k + \mu_i L_i H_u + \frac{1}{2}\lambda''_{ijk} \bar{U}_i \bar{D}_j \bar{D}_k \quad (1)$$

where L and Q are the lepton and quark SU(2) doublet superfields, while $\bar{E}$, $\bar{U}$, and $\bar{D}$ denote the weak isospin singlet fields and the indices i, j, k refer to the fermion families. The coupling strengths in the trilinear terms are given by the Yukawa coupling constants λ, λ' and λ''. Terms appearing in the first line of Eq. (1) violate lepton number by one unit, and the last term in the second line leads to baryon number violation. The bilinear term $\mu_i L_i H_u$ mixes lepton and Higgs (H_u) superfields.

This letter reports on a search for chargino and neutralino pair production under the hypothesis that $\not{R}_p$ can only occur via a term of the type $\lambda_{ijk}\, L_i L_j \bar{E}_k$. A non-zero $\not{R}_p$ coupling λ_{ijk} thus enables a slepton to decay into a lepton pair, as shown in Fig. 1 for the $\not{R}_p$-decay of the lightest neutralino. The so-called $LL\bar{E}$ couplings λ_{ijk} specifically studied here, are λ_{121}, λ_{122}, and λ_{133}. One coupling is assumed to be dominant at a time, with any other $\not{R}_p$-coupling negligibly small.

The initial state at the Fermilab Tevatron Collider consists of hadrons, so the production of a single SUSY particle could only occur through a trilinear term including at least one baryon field, i.e. via λ' or λ'' terms. Since only the $LL\bar{E}$ term (λ) is considered here, an assumption is made that SUSY particles are produced pairwise in an R-parity conserving process [5], with $\not{R}_p$ manifesting itself in the decay only. Even though direct decays of heavy gauginos ($\tilde{\chi}^0_{2,3,4}$, $\tilde{\chi}^\pm_2$) are possible, they predominantly cascade decay into the lightest supersymmetric particle (LSP), which in turn decays into SM particles via $\not{R}_p$. In all scenarios studied here, the lightest neutralino ($\tilde{\chi}^0_1$) is assumed to be the LSP.

Two SUSY models are investigated. In the minimal supergravity model (mSUGRA) [6], the universal soft breaking mass parameter for all scalars at the unification scale, m_0, is set to 100 GeV or 1 TeV. At low m_0, the stau can be lighter than the second lightest neutralino ($\tilde{\chi}^0_2$) and the lightest chargino ($\tilde{\chi}^\pm_1$), leading to a larger number of final states with taus. By contrast, a high value of m_0 prevents complex cascade decays involving sleptons. The universal trilinear coupling, A_0, has only a small influence on the gaugino pair production cross section and is set to zero as in the previous Run I analysis [7]. Searches for supersymmetric Higgs bosons at LEP [8] imply that $\tan\beta \leq 2$ is excluded, where $\tan\beta$ is the ratio of the vacuum expectation values of the two neutral Higgs fields. Since the cross section for gaugino pair production increases with increasing $\tan\beta$ due to decreasing masses, a value of $\tan\beta = 5$ (close to the LEP limit) is chosen to ensure conservative results. A higher value of $\tan\beta = 20$ is studied exclusively in the $ee\tau$ analysis, because the stau mass decreases with increasing $\tan\beta$, leading to an enhanced signal efficiency for this particular analysis. Both signs of the higgsino mixing mass parameter, μ, are considered and the common gaugino mass, $m_{1/2}$, is varied.

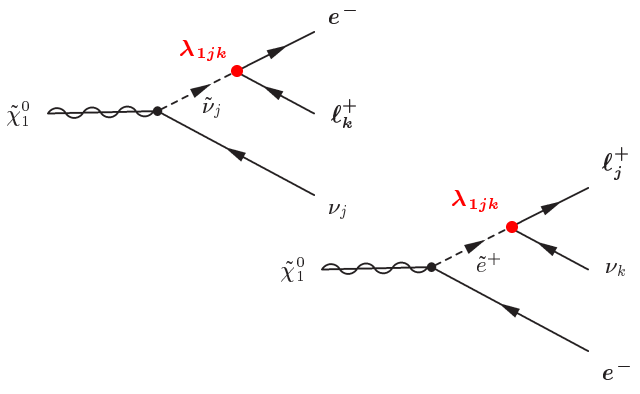

FIG. 1: Two examples of $\not{R}_p$-decays of the lightest neutralino via $LL\bar{E}$ couplings λ_{1jk}. In each decay, two charged leptons and one neutrino are produced.

In the specific minimal supersymmetric standard model (MSSM) [9] considered here, heavy squarks and sleptons (1 TeV) are assumed, while the GUT relation between M_1 and M_2, the masses of the superpartners of

the $U(1)_Y$ and $SU(2)_L$ gauge bosons, is relaxed. The value of $\tan\beta$ is set to 5, and M_1 and M_2 are varied independently. The higgsino mixing mass parameter μ is set to 1 TeV, so that $\tilde{\chi}_3^0$, $\tilde{\chi}_4^0$, and $\tilde{\chi}_2^\pm$ are heavy.

Within the domain of the SUSY parameters explored in this analysis, pair production of $\tilde{\chi}_1^\pm\tilde{\chi}_1^\mp$ and $\tilde{\chi}_2^0\tilde{\chi}_1^\pm$ are the dominant processes, leading to final states with at least four charged leptons and two neutrinos. They come from either the decay of the $\tilde{\chi}_1^0$, with the lepton flavors depending on λ_{ijk}, or from cascade decays of $\tilde{\chi}_1^\pm$ and $\tilde{\chi}_2^0$. The strengths of the couplings are set to 0.01 (λ_{121} and λ_{122}) and 0.003 (λ_{133}). These values are well below the current limits of $\lambda_{121} < 0.5$, $\lambda_{122} < 0.085$, and $\lambda_{133} < 0.005$ for a slepton mass of 1 TeV, which have been derived from the upper limits $\lambda_{121} < 0.05$, $\lambda_{122} < 0.027$, and $\lambda_{133} < 0.0016$ obtained for a slepton mass of 100 GeV in Refs. [4, 10]. Additionally, only neutralinos with a decay length of less than 1 cm are considered, which results in a cut-off at low neutralino masses [11], i.e. 30 GeV for λ_{121} and λ_{122}, and 50 GeV for λ_{133}, again for slepton masses of 1 TeV. As the $\tilde{\chi}_1^0$ can be light, the leptons can have small transverse (w.r.t. the beam axis) momentum and thus be difficult to detect. For this reason, only three charged leptons with the flavor combinations $ee\ell$, $\mu\mu\ell$, or $ee\tau$ ($\ell = e$ or μ) are required.

The analysis is based on a dataset recorded with the DØ detector between April 2002 and August 2004, corresponding to an integrated luminosity of $\mathcal{L} = 360 \pm 23\,\mathrm{pb}^{-1}$. Previous searches with the hypothesis of a $LL\bar{E}$ coupling have been performed by the DØ collaboration with Tevatron Run I data collected at a center-of-mass energy $\sqrt{s} = 1.8$ TeV [7].

The DØ detector consists of a central tracking system surrounded by a uranium/liquid-argon sampling calorimeter and a system of muon detectors [12]. Charged particles are reconstructed using multiple layers of silicon detectors, as well as eight double layers of scintillating fibers in the 2 T axial magnetic field of a superconducting solenoid. The DØ calorimeter provides hermetic coverage up to pseudorapidities $|\eta| = |-\ln[\tan(\theta/2)]| \approx 4$ in a semi-projective tower geometry with longitudinal segmentation. The polar angle θ is measured from the geometric center of the detector with respect to the proton-beam direction. The muon system covers $|\eta| < 2$ and consists of a layer of tracking detectors and scintillation trigger counters in front of 1.8 T toroidal magnets, followed by two more similar layers of detectors outside the toroids [13].

Events containing electrons or muons are selected for offline analysis by a real-time three-stage trigger system. A set of single and dilepton triggers is used to tag the presence of electrons or muons based on their characteristic energy deposits in the calorimeter, the presence of high-momentum tracks in the tracking system, and hits in the muon detectors.

R-parity violating supersymmetry events are modeled using SUSYGEN [14], with CTEQ5L [15] parton distribution functions (PDFs). The package SUSYGEN is interfaced with the program SUSPECT [16] for the evolution of masses and couplings from the renormalization group equations. Leading order (LO) cross sections of signal processes, obtained with SUSYGEN, are multiplied by a K factor computed with GAUGINOS [17]. Standard model processes are generated using the Monte Carlo (MC) generator PYTHIA [18]. All MC events are processed through a detailed simulation of the detector geometry and response based on GEANT3 [19]. Multiple interactions per crossing as well as detector pile-up are included in the simulations. The SM background predictions are normalized using cross section calculations at next-to-leading order (NLO) and next-to-NLO (for Drell-Yan production) with CTEQ6.1M PDFs [20]. Background from multijet production is estimated from data similar to the search samples, however, the lepton identification and isolation criteria are inverted ($ee\ell$ and $ee\tau$) or loosened ($\mu\mu\ell$). These samples are scaled at an early stage of the analysis where multijet production still dominates.

Electrons are identified based on their characteristic energy deposition in the calorimeter. The fraction of energy deposited in the electromagnetic part of the calorimeter and the transverse shower profile inside a cone of radius $\Delta\mathcal{R} = \sqrt{(\Delta\eta)^2 + (\Delta\varphi)^2} = 0.4$ around the cluster direction are considered (where φ is the azimuthal angle). In addition, a track must point to the energy deposition in the calorimeter and its momentum and the calorimeter energy must be consistent with each other. Remaining backgrounds from jets are suppressed based on the track multiplicity within $\Delta\mathcal{R} = 0.4$ around the track direction.

Muons are reconstructed using track segments in the muon system, and each muon is required to have a matched central track measured with the tracking detectors. Furthermore, muons are required to be isolated in both the tracking detectors and the calorimeter, which is essential for rejecting muons associated with heavy-flavor jets. The sum of the track transverse momenta (p_T) inside a cone of $\Delta\mathcal{R} = 0.5$ around the muon direction should be less than 2.5 GeV and less than 6% of the muon p_T. For the calorimeter isolation, a transverse energy (E_T) of less than 2.5 GeV in a hollow cone of $0.1 < \Delta\mathcal{R} < 0.4$ around the muon direction is required and less than 8% of the muon's transverse energy should be deposited in the calorimeter inside this hollow cone. For both isolation criteria, the p_T (E_T) of the muon track itself is excluded from the sum.

Electrons and muons are required to be isolated from each other ($\Delta\mathcal{R}_{e\mu} > 0.2$), among themselves ($\Delta\mathcal{R}_{ee} > 0.4$, $\Delta\mathcal{R}_{\mu\mu} > 0.2$), and from hadronic jets ($\Delta\mathcal{R}_{\ell j} > 0.5$).

Taus decaying hadronically (τ_{had}) are detected as narrow, isolated jets with a specific ratio of electromagnetic to hadronic energy. Two neural networks (NN) are used to identify one-prong tau decays according to the calorimeter information: either with no subclusters in the electromagnetic section of the calorimeter (π-like)

or with EM subclusters (ρ-like) [21]. Muons misidentified as taus are removed by taking the shower shape of the hadronic cluster into account.

Jets are defined using an iterative seed-based cone algorithm [22], clustering calorimeter energy within $\Delta\mathcal{R} = 0.5$. The jet energy calibration is determined from the transverse momentum balance in photon plus jet events. Missing transverse energy ($\not\!\!E_T$) is calculated as the negative vector sum of energy deposits in the calorimeter cells, taking into account energy corrections for reconstructed electrons, muons, and jets.

Electron, muon, and tau reconstruction efficiencies and resolutions are determined using measured Z boson decays. They are parametrized as functions of p_T, η, and ϕ and applied to the simulated MC events. The electron and muon trigger efficiencies are measured in data and translate to signal event trigger efficiencies close to 100% for $ee\ell$ and $ee\tau$, and around 94% for $\mu\mu\ell$.

To achieve the best sensitivity for each $\not\!\!R_p$-coupling, three different analyses are used depending on the flavors of the leptons in the final state: $ee\ell$, $\mu\mu\ell$, and $ee\tau$ ($\ell = e$ or μ). The criteria are summarized in Table I. Each analysis requires three identified leptons with minimum transverse momenta $p_T^{\ell i}$. In the $ee\ell$ and $ee\tau$ analyses, the same lepton quality criteria are applied to each lepton, independent of its transverse momentum. The $\mu\mu\ell$ analysis, however, uses looser quality criteria for the lowest-p_T lepton to increase the selection efficiency. Dielectron and dimuon backgrounds from Drell-Yan, Υ, and Z boson production are suppressed using cuts on $\not\!\!E_T$ and on the invariant dilepton mass $M_{\ell\ell}$ (for the $\mu\mu\ell$ and $ee\tau$ analyses). All three analyses are optimized separately using SM and signal MC simulations.

Cuts I and II of the $ee\ell$ analysis (Table I) are used to select a dielectron control sample for data and MC comparison, while cuts III and IV define the trilepton $ee\ell$ analysis. Cut III requires three leptons to be identified, two of which must be electrons. Cut IV, the photon conversion veto, which requires that a track associated with an electron has hits in the innermost layers of the silicon detector, is extended to all identified electrons in an event. Contrary to this, cut II only applies to the two electrons of the control sample. In the $\mu\mu\ell$ and $ee\tau$ analyses all cuts presented in Table I serve as selection cuts for the respective trilepton sample and are applied successively to all MC samples and the data. Two-dimensional cuts in the ($\not\!\!E_T$, $M_{\mu\mu}$) and ($\Delta\varphi(\mu\mu)$, $\not\!\!E_T$) planes are defined in the $\mu\mu\ell$ analysis to veto events from Υ and Z boson production. In the $ee\tau$ analysis, hadronic tau decays are identified by requiring the transverse energy deposited in a calorimeter cone of radius $\Delta\mathcal{R} = 0.5$ to be above 10 GeV and an NN output of more than NN > 0.9, corresponding to cut III in Table I. To select events with real $\not\!\!E_T$, which is expected due to neutrinos in the final state, a cut on $\not\!\!E_T/\sqrt{S_T}$ is applied, where S_T is the total scalar transverse energy. It allows discrimination against events with fake $\not\!\!E_T$, which may arise through statistical fluctuations in jet energy measurements.

TABLE I: Summary of the selection criteria for $ee\ell$, $\mu\mu\ell$, and $ee\tau$ analyses and numbers of events observed in data and expected from SM background, including statistical and systematic uncertainties.

	$ee\ell$ ($\ell = e$ or μ) analysis		
	Cut	Data	Background
I	$p_T^{e1} > 20$ GeV, $p_T^{e2} > 20$ GeV	20170	$20534 \pm 55 \pm 1484$
II	γ-conversion veto (lead. 2 e) and $\not\!\!E_T > 15$ GeV	1247	$1241 \pm 21 \pm 668$
III	$p_T^{\ell 1} > 20$ GeV, $p_T^{\ell 2} > 20$ GeV $p_T^{\ell 3} > 10$ GeV, at least 2 e	5	$5.5^{+0.8}_{-0.5} \pm 0.6$
IV	γ-conversion veto (all e) and $\not\!\!E_T > 15$ GeV	0	$0.9^{+0.4}_{-0.1} \pm 0.1$
	$\mu\mu\ell$ ($\ell = \mu$ or e) analysis		
	Cut	Data	Background
I	$p_T^{\ell 1} > 12$ GeV, $p_T^{\ell 2} > 8$ GeV	19283	$19588 \pm 81 \pm 3332$
II	$\Delta\varphi(\mu_i, \not\!\!E_T) > 0.1$	14918	$15275 \pm 72 \pm 2598$
III	Υ and Z veto ($\not\!\!E_T$, $M_{\mu\mu}$) plane $\Delta\varphi(\mu\mu) < 2.53$ for $\not\!\!E_T < 44$ GeV	564	$506 \pm 13 \pm 86$
IV	$p_T^{\mu 3} > 4$ GeV or $p_T^{e} > 5$ GeV $\Delta\varphi(e, \not\!\!E_T) > 0.1$ $\sum p_T^{\ell i} > 50$ GeV	0	$0.4 \pm 0.1 \pm 0.1$
	$ee\tau$ analysis		
	Cut	Data	Background
I	$p_T^{e1} > 10$ GeV, $p_T^{e2} > 10$ GeV $M_{ee} > 18$ GeV	20437	$20905 \pm 70 \pm 1555$
II	$M_{ee} < 80$ GeV	2831	$2531 \pm 32 \pm 329$
III	τ: $E_T > 10$ GeV, NN > 0.9	16	$11.0 \pm 2.8 \pm 2.0$
IV	$\not\!\!E_T/\sqrt{S_T} > 1.5$ GeV$^{1/2}$	0	$1.3 \pm 1.7 \pm 0.5$

Figure 2 shows (a) the dielectron invariant mass in the $ee\ell$ analysis after cut I of Table I, (b) the missing transverse energy distribution in the $\mu\mu\ell$ analysis after cut III of Table I, and (c) the neural network output for a loose $Z \to \tau\tau \to \tau_{had}\mu$ selection, which is used as an identification criterion for taus in the $ee\tau$ analysis. The μ+jet opposite-sign data sample (OS) represents the control sample, while the μ+jet like-sign data sample (LS) is used to model the multijet background. The different contributions are scaled to the control sample by fitting the E_T spectrum of the tau candidate. While in (a,b) the signal is scaled by a factor of 50, an arbitrary scale is used in (c), since the search and control samples are completely independent of each other and no meaningful scale can be defined for the signal contribution w.r.t. $Z \to \tau\tau$ or μ+jet data.

The number of observed events in data and the expected background from SM processes with its respective statistical and systematic uncertainties are given in Table I. The multijet background, expressed as a fraction of the SM background, is 11±7%, below 1% and 15±15% in the $ee\ell$, $\mu\mu\ell$, and $ee\tau$ analyses, respectively. The number of events observed in data is in good agreement with the expectation from SM processes at all stages of the three analyses.

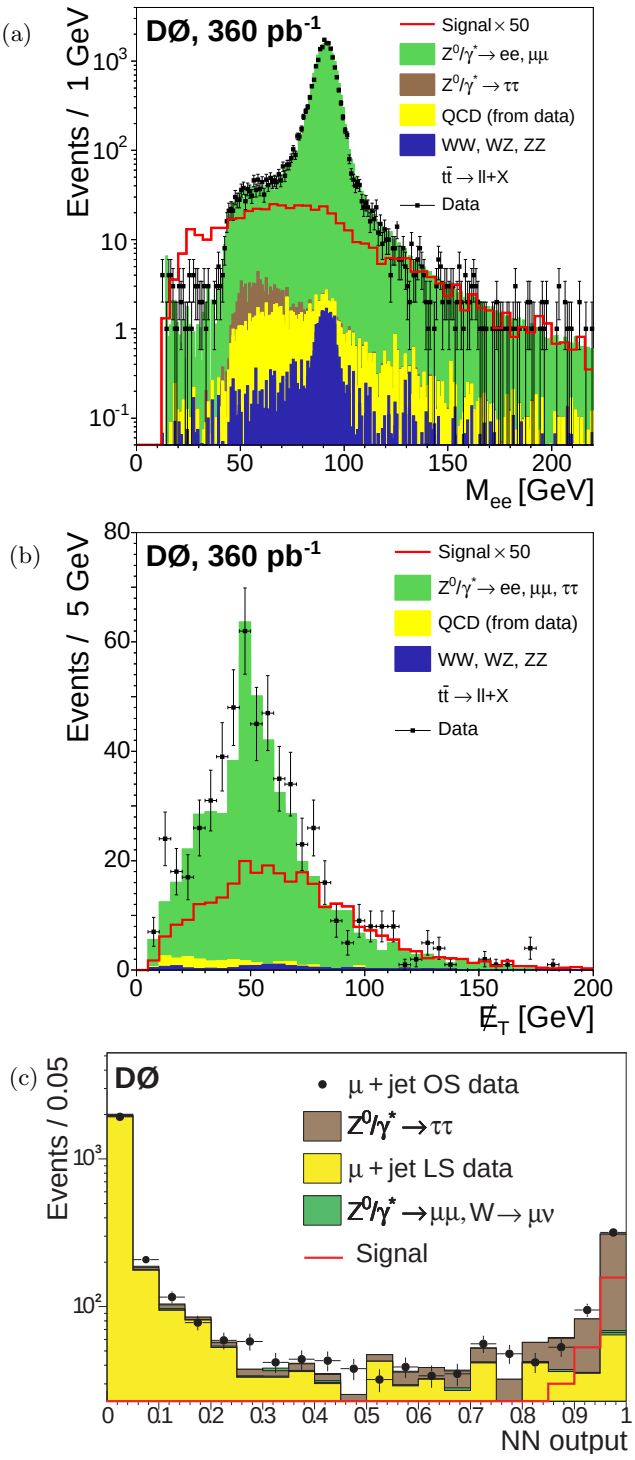

FIG. 2: (a) The dielectron invariant mass distribution of the $ee\ell$ analysis after cut I, Table I; (b) the $\not\!\!E_T$ distribution of the $\mu\mu\ell$ analysis after cut III, Table I; and (c) the combination of the π and ρ-like NN outputs of a loose $Z \to \tau\tau \to \tau_{had}\mu$ selection used as the τ identification criterion in the $ee\tau$ analysis. In (c) like-sign (opposite-sign) μ+jet data is abbreviated LS (OS) and signal refers to the mSUGRA point $m_0 = 1$ TeV, $\tan\beta = 5$, $\mu > 0$, $A_0 = 0$, and $m_{1/2} = 280$ GeV, scaled by a factor of 50 in (a,b) and arbitrarily in (c), details in the text.

The numbers of events expected from SM background and from signal depend on several quantities, each one introducing a systematic uncertainty. The relative uncertainty due to the luminosity measurement is 6.5%. The relative uncertainty on trigger efficiencies ranges from about 11% for Drell-Yan (DY) background with low dilepton invariant masses (15 GeV $< M_{\ell\ell} <$ 60 GeV) to about 1% for the signal. Lepton identification and reconstruction efficiencies give 3% (e), 4% (μ), and 12% (τ) per lepton candidate, and the photon conversion veto adds another 0.4%. The relative systematic uncertainties due to the resolution of the electron or muon energies and $\not\!\!E_T$ are estimated by varying the resolutions in the MC simulation and are found to be less than 1% (e), 1.5% (μ), and 2% ($\not\!\!E_T$).

Further systematic uncertainties on the experimental cross section limits concern the theoretical uncertainties on SM background MC cross sections, ranging from 3% to 17%, depending on the process, and including PDF uncertainties. Since PYTHIA does not model the Z boson p_T accurately, a relative uncertainty of 3% to 15%, depending on the dilepton mass, is added for MC Drell-Yan events. The influence of PDF uncertainties on the signal acceptance is estimated to be 4%.

Theoretical uncertainties on the signal cross sections are due to variations of the renormalization and factorization scales (5%), the LO cross section (2%), the K factor (3%), and the choice of PDF (9%). As gaugino pair production mostly proceeds via s-channel exchange of virtual γ, W, or Z bosons, the latter uncertainty is deduced from studies of the DY cross section at similar masses. The uncertainty on the DY cross section due to the choice of PDF is estimated to be 6%, using the CTEQ6.1M uncertainty function set [20]. An additional 3% is added linearly to account for the lower DY cross section if calculated with CTEQ6 PDFs, compared to its estimation with CTEQ5 PDFs, which are used for the signal MC generation. An additional, conservative, systematic uncertainty of $+10/-0$% is added to account for the lower LO cross section from SUSYGEN compared to the one obtained with PYTHIA. All of these uncertainties are assumed to be independent, and are added in quadrature. The total systematic uncertainty of -11% and $+15$% is represented by the grey-shaded bands of the signal cross section curve in Fig. 3.

When setting limits, the $ee\ell$, $\mu\mu\ell$, and $ee\tau$ analyses are combined for each coupling (λ_{121}, λ_{122}, λ_{133}) in order to enhance the signal sensitivity. All signal and background samples, as well as the data are processed by all analyses according to the three channels. Events selected in multiple channels are assigned only to the analysis with the largest signal-to-background ratio, and are removed from all other analyses. The percentage of common signal events for any two analyses is less than 13%, while no common data or SM background events are found. Table II shows the efficiencies of the analyses for a typical mSUGRA point ($m_0 = 1$ TeV, $\tan\beta = 5$, $\mu > 0$, $A_0 = 0$,

and $m_{1/2} = 280$ GeV). Correlations between the signal efficiencies in the three channels are taken into account in the calculation of the systematic uncertainties.

TABLE II: Efficiencies (in %) of the $ee\ell$, $\mu\mu\ell$, and $ee\tau$ analyses and of the combined analyses for a typical mSUGRA point ($m_0 = 1$ TeV, $\tan\beta = 5$, $\mu > 0$, $A_0 = 0$, and $m_{1/2} = 280$ GeV). The first uncertainty is statistical and the second one systematic.

Analysis	λ_{121}	λ_{122}	λ_{133}
$\varepsilon(ee\ell)$	$18.9 \pm 0.3 \pm 1.2$	$4.5 \pm 0.2 \pm 0.3$	$2.6 \pm 0.2 \pm 0.1$
$\varepsilon(\mu\mu\ell)$	$2.1 \pm 0.1 \pm 0.3$	$16.1 \pm 0.1 \pm 1.9$	$0.8 \pm 0.1 \pm 0.1$
$\varepsilon(ee\tau)$	$1.1 \pm 0.1 \pm 0.1$	$0.23 \pm 0.04 \pm 0.03$	$2.0 \pm 0.2 \pm 0.2$
ε_{comb}	$22.1 \pm 0.3 \pm 1.6$	$20.8 \pm 0.2 \pm 2.2$	$5.4 \pm 0.3 \pm 0.4$

Since no evidence for gaugino pair production is observed, upper limits on the cross sections are extracted in two models: in mSUGRA (with $m_0 = 100$ GeV or 1 TeV, $\tan\beta = 5$ or 20, $\mu > 0$, and $A_0 = 0$) and in an MSSM model assuming no GUT relation between M_1 and M_2 and assuming heavy squarks and sleptons, i.e. the higgsino mixing mass parameter, μ, and all sfermion masses are set to 1 TeV. Limits are calculated at the 95% C.L. using the LEP CL_S method [23] taking into account correlated uncertainties between SM and signal processes.

For mSUGRA ($m_0 = 1$ TeV and $\tan\beta = 5$), the expected and observed cross section limits ($\sigma_{95\%CL}$) are shown in Fig. 3 as functions of the $\tilde{\chi}_1^0$ and $\tilde{\chi}_1^\pm$ masses.

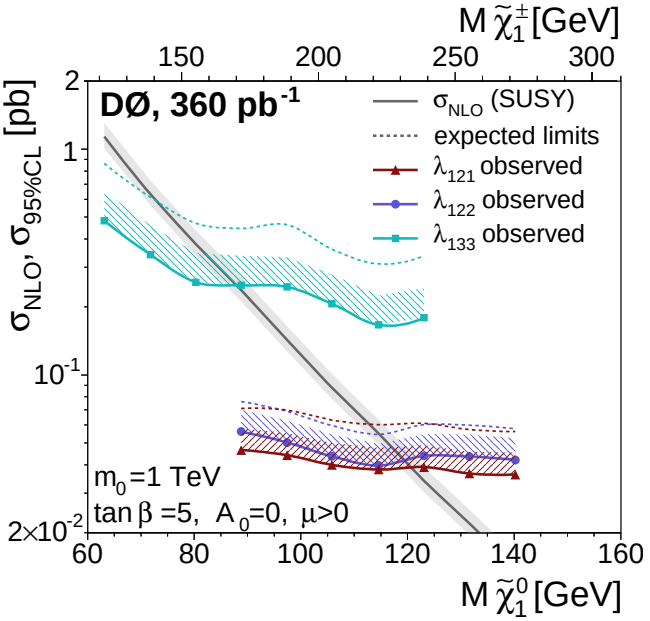

FIG. 3: mSUGRA ($m_0 = 1$ TeV, $\tan\beta = 5$, $\mu > 0$, $A_0 = 0$): The σ_{NLO} cross section and the $\sigma_{95\%CL}$ limits for the λ_{121}, λ_{122}, and λ_{133} analyses as functions of the $\tilde{\chi}_1^0$ mass (lower horizontal axis) and the $\tilde{\chi}_1^\pm$ mass (upper horizontal axis). The exclusion domains, indicated by the hatched regions, lie above the respective observed limit curve.

Studies for $m_0 = 100$ GeV and $\tan\beta = 5$ and 20 are done for λ_{133}. Particularly interesting is the region of high $\tan\beta$ values, where the stau is the next-to-lightest supersymmetric particle. In such a case, decays of SUSY particles into final states with stau leptons can be dominant and consequently increase the efficiency of the $ee\tau$ channel. Lower bounds on the masses of the $\tilde{\chi}_1^0$ and the $\tilde{\chi}_1^\pm$ are given in Table III.

In the MSSM, the exclusion domain is presented in the ($\tilde{\chi}_1^0$, $\tilde{\chi}_1^\pm$) mass plane in Fig. 4. The cut-off of the exclusion domain towards low neutralino masses, i.e. at $m_{\tilde{\chi}_1^0} = 30$ GeV for λ_{121} and λ_{122}, and at $m_{\tilde{\chi}_1^0} = 50$ GeV for λ_{133}, is due to the combined effect of the mean decay length of the lightest neutralino (chosen to lie below one cm) and the values of the λ_{121}, λ_{122}, and λ_{133} couplings.

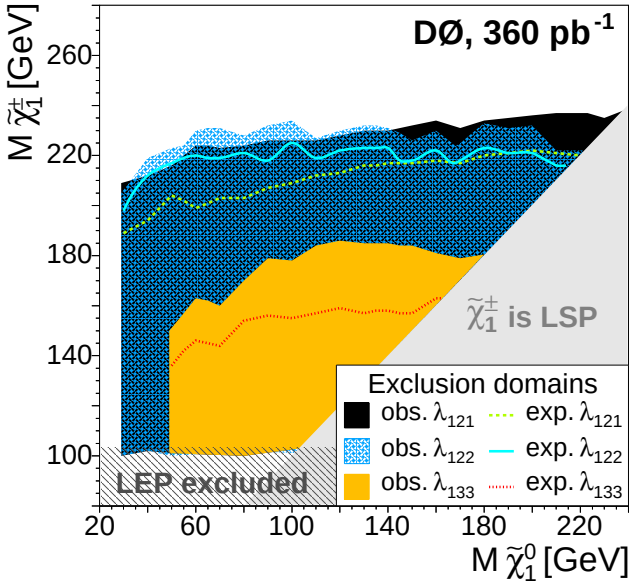

FIG. 4: Observed and expected exclusion domains at the 95% C.L. in the ($\tilde{\chi}_1^0$, $\tilde{\chi}_1^\pm$) mass plane of the considered MSSM model for the λ_{121}, λ_{122}, and λ_{133} couplings with their strengths set to 0.01 (λ_{121}, λ_{122}) and 0.003 (λ_{133}).

TABLE III: The combined lower limits at the 95% C.L. on the masses of $\tilde{\chi}_1^0$ and $\tilde{\chi}_1^\pm$ (in GeV) obtained using the mSUGRA model with different parameters.

Coupling	sign(μ)	$m(\tilde{\chi}_1^0)$	$m(\tilde{\chi}_1^\pm)$
λ_{121} ($m_0 = 1$ TeV, $\tan\beta = 5$)	> 0	119	231
λ_{122}	> 0	118	229
λ_{133}	> 0	86	166
λ_{121} ($m_0 = 1$ TeV, $\tan\beta = 5$)	< 0	117	234
λ_{122}	< 0	115	230
λ_{133} ($m_0 = 100$ GeV, $\tan\beta = 5$)	> 0	105	195
λ_{133} ($m_0 = 100$ GeV, $\tan\beta = 20$)	> 0	115	217

In summary, no evidence for R_p-SUSY is observed in trilepton events. Upper limits on the chargino and neutralino pair production cross section are set in the

case of one dominant coupling: λ_{121}, λ_{122}, or λ_{133}. Lower bounds on the masses of the lightest neutralino and the lightest chargino are derived in mSUGRA and in an MSSM scenario with heavy sfermions, but assuming no GUT relation between M_1 and M_2. All limits significantly improve previous results obtained at LEP [4] and with the DØ Run I dataset [7] and are the most restrictive to date.

We wish to thank M. Klasen for providing us with the GAUGINOS package for the calculation of the K factors for the SUSY signal. We thank the staffs at Fermilab and collaborating institutions, and acknowledge support from the DOE and NSF (USA); CEA and CNRS/IN2P3 (France); FASI, Rosatom and RFBR (Russia); CAPES, CNPq, FAPERJ, FAPESP and FUNDUNESP (Brazil); DAE and DST (India); Colciencias (Colombia); CONACyT (Mexico); KRF and KOSEF (Korea); CONICET and UBACyT (Argentina); FOM (The Netherlands); PPARC (United Kingdom); MSMT (Czech Republic); CRC Program, CFI, NSERC and WestGrid Project (Canada); BMBF and DFG (Germany); SFI (Ireland); The Swedish Research Council (Sweden); Research Corporation; Alexander von Humboldt Foundation; and the Marie Curie Program.

---

[*] On leave from IEP SAS Kosice, Slovakia.
[†] Visitor from Helsinki Institute of Physics, Helsinki, Finland.

[1] Y.A. Golfand and E.P. Likhtman, JETP Lett. 13 (1971) 323; D.V. Volkov and V.P. Akulov, JETP Lett. 16 (1972) 438; D.V. Volkov and V.P. Akulov, Phys. Lett. 46 B (1973) 109; J. Wess and B. Zumino, Nucl. Phys. B 70 (1974) 39.
[2] P. Fayet, Phys. Lett. 69 B (1977) 489;
P. Fayet, Phys. Lett. 70 B (1977) 461.
[3] G. Farrar and P. Fayet, Phys. Lett. 76 B (1978) 575;
H.K. Dreiner, in *Perspectives on Supersymmetry*, Ed. G.L. Kane, World Scientic, Singapore, (1998), p. 462; arXiv: hep-ph/9707435.
[4] R. Barbier et al., Phys. Rept. 420 (2005) 1, and references therein.
[5] SUGRA Working Group Collaboration, S. Abel et al., arXiv: hep-ph/0003154 (part 2) and R-parity Working Group Collaboration, B. Allanach et al., arXiv: hep-ph/9906224 (part 4) in Proceedings of *Physics at Run II: Workshop On Supersymmetry / Higgs*, Eds. M. Carena and J.D. Lykken, FERMILAB-PUB-00-349, (2000).
[6] H.P. Nilles, Phys. Rept. 110 (1984) 1.
[7] DØ Collaboration, B. Abbott et al., Phys. Rev. D 62 (2000) 071701.
[8] ALEPH, DELPHI, L3 and OPAL Collaborations and the LEP Working Group for Higgs Boson Searches, submitted to Eur. Phys. J.C, arXiv:hep-ex/0602042.
[9] H.E. Haber and G.L. Kane Phys. Rept. 117 (1985) 75.
[10] F. Ledroit and G. Sajot, Rapport GDR-Supersymétrie GDR-S-008, ISN Grenoble, (1998).
[11] S. Dawson, Nucl. Phys. B 261 (1985) 297.
[12] DØ Collaboration, V.M. Abazov et al., submitted to Nucl. Instrum. Methods Phys. Res. A, arXiv:physics/0507191.
[13] V.M. Abazov et al., Nucl. Instrum. Methods Phys. Res. A 552 (2005) 372.
[14] N. Ghodbane, S. Katsanevas, P. Morawitz, and E. Perez, SUSYGEN 3, arXiv: hep-ph/9909499; `http://lyoinfo.in2p3.fr/susygen/susygen3.html`.
[15] H.L. Lai et al., Eur. Phys. J.C 12 (2000) 375.
[16] A. Djouadi, J-L. Kneur and G. Moultaka, SUSPECT, arXiv: hep-ph/0211331, (2002); version: SUSPECT 2.2.
[17] W. Beenakker et al. Phys. Rev. Lett. 83 (1999) 3780.
[18] T. Sjöstrand et al., Comput. Phys. Commun. 135 (2001) 238; with L. Lönnblad, *PYTHIA 6.2 Physics and Manual*, arXiv:hep-ph/0108264; versions: PYTHIA 6.201 and PYTHIA 6.202.
[19] R. Brun and F. Carminati, CERN Program Library Long Writeup W5013 (1993).
[20] J. Pumplin et al., JHEP 0207 (2002) 012;
D. Stump et al., JHEP 0310 (2003) 046.
[21] DØ Collaboration, V. Abazov et al., Phys. Rev. D 71 (2005) 072004.
[22] G. Blazey et al., Proceedings of the workshop *"QCD and Weak Boson Physics in Run II"*, Eds. U. Baur, R.K. Ellis and D. Zeppenfeld, Batavia (2000), p.47.
[23] T. Junk, Nucl. Instrum. Methods Phys. Res. A 434 (1999) 435.